Light-phase prednisone promotes glucose oxidation in heart through novel transactivation targets of cardiomyocyte-specific GR and KLF15

Authors: Fadoua El Abdellaoui Soussi[1#], Hima Bindu Durumutla[1#], Hannah Latimer[1], Ashok Daniel Prabakaran[1], Kevin McFarland[1], Karen Miz[1], Kevin Piczer[1], Cole Werbrich[1], Mukesh K Jain[2], Saptarsi M Haldar[3], Mattia Quattrocelli[1,*]

[#] These Authors contributed equally

Affiliations:

[1] Molecular Cardiovascular Biology, Heart Institute, Cincinnati Children's Hospital Medical Center and Dept. Pediatrics, University of Cincinnati College of Medicine, Cincinnati, OH, USA;

[2] Dept Cell Biology and Biochemistry, Brown University, Providence, RI, USA;

[3] Amgen Research, South San Francisco, CA, USA; Gladstone Institutes, San Francisco, CA, USA and Dept Medicine, Cardiology Division, UCSF, San Francisco, CA, USA

*** Corresponding Author:** Mattia Quattrocelli, PhD, Molecular Cardiovascular Biology, Heart Institute, Cincinnati Children's Hospital Medical Center, 240 Albert Sabin Way T4.676, Cincinnati, OH 45229.
Email: mattia.quattrocelli@cchmc.org, tel: +1-513-517-1221.

Keywords – Glucocorticoids, prednisone, chrono-pharmacology, glucose uptake, pyruvate oxidation, Adipor1, mitochondrial pyruvate carrier, glucocorticoid receptor, KLF15.

Data availability - RNA-seq and ChIP-seq datasets reported here will be available upon completion of the peer-review process.

Conflicts of interest – MQ is listed as co-inventor on a patent application related to intermittent glucocorticoid use filed by Northwestern University (PCT/US2019/068,618). All other authors declare they have no competing interests.

ABSTRACT

Circadian time of intake determines the cardioprotective outcome of glucocorticoids in normal and infarcted hearts. The cardiomyocyte-specific glucocorticoid receptor (GR) is genetically required to preserve normal heart function in the long-term. The GR co-factor KLF15 is a pleiotropic regulator of cardiac metabolism. However, the cardiomyocyte-autonomous metabolic targets of the GR-KLF15 concerted epigenetic action remain undefined. Here we report that circadian time of intake determines the activation of a transcriptional and functional glucose oxidation program in heart by the glucocorticoid prednisone with comparable magnitude between sexes. We overlayed transcriptomics, epigenomics and cardiomyocyte-specific inducible ablation of either GR or KLF15. Downstream of a light-phase prednisone stimulation in mice, we found that both factors are non-redundantly required in heart to transactivate the adiponectin receptor expression (*Adipor1)* and promote insulin-stimulated glucose uptake, as well as transactivate the mitochondrial pyruvate complex expression *(Mpc1/2)* and promote pyruvate oxidation. We then challenged this time-specific drug effect in obese diabetic *db/db* mice, where the heart shows insulin resistance and defective glucose oxidation. Opposite to dark-phase dosing, light-phase prednisone rescued glucose oxidation in *db/db* cardiomyocytes and diastolic function in *db/db* hearts towards control-like levels with sex-independent magnitude of effect. In summary, our study identifies novel cardiomyocyte-autonomous metabolic targets of the GR-KLF15 concerted program mediating the time-specific cardioprotective effects of glucocorticoids on cardiomyocyte glucose utilization.

INTRODUCTION

Glucose oxidation is an important fuel source for the heart and is generally impaired in heart failure with either reduced or preserved ejection fraction[1]. A notable context of heart failure that underscores the cardioprotective nature of glucose oxidation is the diabetic heart. The intricate pathogenesis of type-2 diabetic cardiomyopathy involves insulin resistance and impaired glucose oxidation [2], promoting diastolic dysfunction and heightened vulnerability to ischemia [2, 3]. The impact of this metabolic derangement on type-2 diabetic patients is notable as they face a 74% increased risk of developing heart failure, and heart failure in these patients increases their mortality by four-fold [4]. Indeed, despite therapeutic advancements and lifestyle interventions, cardiovascular disease still contributes to half of the fatalities among individuals living with type-2 diabetes [5-7]. Therefore, novel pharmacological targets and strategies to improve cardiac glucose oxidation could be of potential impact for the diabetic heart.

Addressing the multifaceted metabolic aberrations associated with chronic metabolic disorders, including obesity and T2D, poses a formidable challenge necessitating innovative strategies. Metabolic stress in these conditions manifests through NAD+ depletion, an elevation in Acetyl-CoA ratio [8], insulin resistance, and impaired glucose oxidation [9, 10]. This complex milieu underscores the absence of specific and efficacious therapeutic modalities for chronic metabolic disorders at large, and DCM in particular. Traditional therapeutic approaches targeting hemodynamics or neurohormonal signaling have proven ineffective in ameliorating mortality rates. Indeed, the treatment paradigm for DCM often relies on interventions at advanced stages or palliative measures for heart failure [8]. The intricate nature of metabolic dysregulation in DCM underscores the imperative for novel therapeutic approaches that address the underlying molecular perturbations to improve clinical outcomes.

In this context, the glucocorticoid receptor (GR), activated by glucocorticoids (GCs), emerges as a crucial metabolic regulator exerting profound influence on cardiac function [11]. Specific cardiac GR knockout models demonstrate that insufficiency in GR functionality leads to cardiac dysfunction, thereby establishing the pathogenic nature of deficient GR signaling in cardiomyocytes, affecting both contractility through calcium channels regulation and cardiac β-adrenergic signaling [12]. Conversely, human GR overexpression in the heart does not significantly alter the heart function but induces changes in L-type calcium channels, accompanied by reductions in Na+ and K+, with bradycardia and atrioventricular blocks as an ultimate physiological consequence [13]. These findings emphasize the intricate role of GR in cardiac physiology and homeostasis.

Recent studies unveil two temporal dimensions within GC pharmacology: circadian time-of-intake and chronic frequency-of-intake. Light-phase dosing of prednisone demonstrated benefits, contrasting with deleterious effects observed with dark-phase dosing [14]. Intermittent once-weekly prednisone dosing showed promise in reversing dysmetabolic effects [15]. Pilot clinical trials involving circadian-restricted intermittent prednisone in

dystrophic patients supported feasibility and relevance for humans [16]. Initial findings in obese diabetic mice suggest a potential repurposing of GC drugs to alleviate DCM. This is further supported by studies elucidating the pivotal role of circulating hormones, acting through GR, in the regulation of peripheral circadian clocks [17], highlighting the link between circadian rhythm dysregulation and heightened risk of myocardial infarction. However, the cardiomyocyte-autonomous role of GR in heart metabolism remains elusive, constituting a gap in current understanding [11, 18]. Notably, the GR is intricately linked to the circadian rhythm, with its activity being subject to regulation by the circadian clock [19, 20]. The circadian clock factor BMAL1, recognized for its essential role in NAD+ repletion and cardiac function, raises questions about its response to GC signaling within the heart [21, 22].

Kruppel-like factor 15 (KLF15), a member of the zinc finger transcription factor family has emerged as an important regulator of cardiac metabolism and function in the heart. KLF15 has profound influence on cardiac metabolism as it orchestrates the expression of key genes involved in glucose and lipid metabolism, thereby playing a critical role in maintaining energy homeostasis within the myocardium [23]. Additionally, KLF15 has been implicated in the dynamic regulation of gene expression throughout the cardiac circadian cycle, highlighting its involvement in temporal transcriptional programs in the heart [24, 25]. Despite its established role in cardiac transcriptional control and its importance in metabolic responses to stress, KLF15 functions as one of the downstream targets of GR signaling [26]. Notably, GR and KLF15 are reported to cooperate epigenetically; however, the precise mechanisms and coordinated actions of GR and KLF15 in the myocardium downstream of GR signaling remain elusive.

Our study aims to unravel the intricacies of the GC-GR axis in diabetic cardiomyopathy. Leveraging cardiomyocyte-specific inducible knockout models, we explore the circadian and chronic dimensions of GC intake. Preliminary findings with obese diabetic mice suggest a potential repurposing of GC drugs to alleviate diabetic cardiomyopathy, opening new avenues for investigation. Furthermore, building on insights from cardiomyocyte-restricted inducible knockout models, we propose a novel GR-KLF15 mechanism governing clock and metabolism in cardiomyocytes, hypothesizing its role in rescuing DCM in type-2 diabetes. Our results delve into the cardiomyocyte-specific role of GR and KLF15 in heart metabolism, the influence of circadian time-of-intake on GC action, and the novel concept of chronic frequency-of-intake, shedding light on potential breakthroughs in the treatment of diabetic cardiomyopathy.

MATERIAL AND METHODS

Animal handling and treatments

Mice were housed in a pathogen-free facility in accordance with the American Veterinary Medical Association (AVMA) and under protocols fully approved by the Institutional Animal Care and Use Committee (IACUC) at the Cincinnati Children's Hospital Medical Center (#2023-0002). Consistent with the ethical approvals, all efforts were made to minimize suffering. Euthanasia was performed through carbon dioxide inhalation followed by cervical dislocation and heart removal.

Mice were maintained on a 12h/12h light/dark cycle, and diet/pharmacological treatments were initiated at ~ 12 weeks of age. Mice were obtained and interbred from the Jakson Laboratories (Bar Harbor, ME; JAX strain number listed) or from collaborators: WT C57BL/6 mice #000664, Myh6-MerCreMer mice #005657, GR-flox mice #021021, Klf15-flox mice #029787 (provided by Dr. Jain, Brown U), db/db #000642; KLF15-3xFLAG mice [27] were provided by Dr. Haldar (Amgen & UCSF). Gene ablation was induced with tamoxifen right before the start of drug treatments using a combination of i.p. (20 mg/kg/day for 5 days; Sigma #T5648) and chow-mediated (40mg/kg for 3 weeks until 7 days prior to start; Harlan #TD.130,860) administration. Analyses were performed after 7 days of tamoxifen washout. Weekly prednisone treatment consisted of once-weekly intraperitoneal injection of prednisone (1 mg/kg; #P6254, Sigma-Aldrich, St. Louis, MO). The injectable solution was diluted from a stock (5 mg/ml) in dimethyl sulfoxide (DMSO; #D2650, Sigma-Aldrich, St. Louis, MO) in a 50-µl volume. Injections were conducted either at the beginning of the light phase (ZT0; lights on) or at the beginning of the dark phase (ZT14; lights off). Tissues were harvested 24 hours after a single pulse or last injection in chronic treatment. All in vivo, ex vivo, and postmortem analyses were conducted blinded to treatment group.

RNA-seq and qPCR analyses

RNA-seq was conducted on RNA extracted from left ventricle myocardial tissue. Each heart was immediately snap frozen in 1ml TRIsure (Bioline, BIO-38033) using liquid nitrogen. RNAs from each heart were re-purified using RNeasy Mini Kit (Cat #74104; Qiagen, Germantown, MD). RNA-seq was performed at the DNA Core (CCHMC). 150 ng – 300 ng of total RNA determined by Qubit (Cat #Q33238; Invitrogen, Waltham, MA) high-sensitivity spectrofluorometric measurement was poly-A selected and reverse transcribed using Illumina's TruSeq stranded mRNA library preparation kit (Cat# 20020595; Illumina, San Diego, CA). Each sample was fitted with one of 96 adapters containing a different 8 base molecular barcode for high level multiplexing. After 15 cycles of PCR amplification, completed libraries were sequenced on an Illumina NovaSeqTM 6000, generating 20 million or more high quality 100 base long paired end reads per sample. A quality control check on the fastq files was performed using FastQC. Upon passing basic quality metrics, the reads were trimmed to remove adapters and low-quality reads using default parameters in Trimmomatic [Version 0.33]. In the next step, transcript/gene abundance was determined using kallisto [Version 0.43.1]. The trimmed reads were then

mapped to mm10 reference genome using default parameters with strandness (R for single-end and RF for paired-end) option in Hisat2 [Version 2.0.5]. In the next step, transcript/gene abundance was determined using kallisto [Version 0.43.1]. We first created a transcriptome index in kallisto using Ensembl cDNA sequences for the reference genome. This index was then used to quantify transcript abundance in raw counts and counts per million (CPM). Differential expression (DE genes, FDR<0.05) was quantitated through DESeq2. PCA was conducted using ClustVis. Gene ontology pathway enrichment was conducted using the Gene Ontology analysis tool.

Total RNA was extracted from cryo-pulverized liver tissue and hiPSC-derived hepatocyte-like cells using Trizol (Thermo Fisher Scientific) and 1 ug RNA was reverse-transcribed using SuperScript™ IV VILO™ Master Mix (#11756050, Thermo Fisher Scientific). RT-qPCRs were conducted in three replicates using 1X SYBR Green Fast qPCR machine (Bio-Rad, Hercules, CA; thermal profile: 95C, 15 sec; 60C, 30sec; 40x; melting curve). The 2-ΔΔCT method was used to calculate relative gene expression. GAPDH was used as the internal control. Primers were selected among validated primer sets from MGH PrimerBank as follows:

Gene	**Forward**	**Reverse**
Klf15	GAGACCTTCTCGTCACCGAAA	GCTGGAGACATCGCTGTCAT
Adipor1	TCTTCGGGATGTTCTTCCTGG	TTTGGAAAAAGTCCGAGAGACC
Mpc1	CTCCAGAGATTATCAGTGGGCG	GAGCTACTTCGTTTGTTACATGGC
Mpc2	CTCAGTCCACTGTGTTGATGGC	ATCCGAAACAGCTGAGAGGCTC

Mass-spec analysis of ceramides in myocardial tissue

Untargeted lipidomics was performed on myocardial tissue from mice treated for 12-week-long intermittent treatments with vehicle or weekly prednisone. Whole hearts were snap-frozen and then ground to powder with dry ice-chilled mortar and pestle. Frozen samples were sent on dry ice to mass spectrometry Core at the Cincinnati Children's Hospital Medical Center, where LC-MS and data analysis were performed. Briefly 10 µl sample was added to 30 µl of internal standard, except for the blank calibrator. Then 300 µl of Butanol/Methanol (3:1) was added to sample aliquot tube and vortexed for 10 mins. Next, 150 µl of Heptane/Ethyl Acetate (3:1) was added to the sample tube and vortexed for 5 mins. The contents of the sample aliquot were then transferred to a large glass tube, to which 150 µl of Heptane/Ethyle Acetate was added and vortexed for 5 mins. Then, 300 ul of 1% Acetic acid was added to the original tube to wash, vortexed for 5 mins and then added back to the glass tube. The glass tube was further vortexed for 5 mins and let sit for 5 mins. The upper organic phase of ~ 200 µl was transferred to a new glass tube. To this, 320 µl Heptane/Ethyl Acetate (3:1) was added to the water phase, vortexed for 5 mins and let sit for 5 mins. Next, 280

µl of upper organic phase (second extract) was transferred to the first extract. This step is repeated once. The upper organic phase (third extract) of 100 µl was combined with other extracts and dried down with nitrogen in a heating block set to 40°C. The resuspended lipid extracts (2 µl) were loaded and separated through Xevo QTOF G2-S mass spectrometer (Waters Corp). All calculations were performed using QuanLynx.

Chromatin immunoprecipitation sequencing

Whole hearts were cryopowdered using a liquid nitrogen-cooled RETSCH Cryomill. The cryopowdered tissue was then fixed in 10 ml of 1% paraformaldehyde (PFA) for 30 min at room temperature with gentle nutation. Fixation was quenched 1 ml of 1.375 M glycine (Cat# BP381-5, Thermo Fisher Scientific, Waltham, MA) with gentle nutation for 5 mins at room temperature. After centrifugation at 3,000*g* for 5 mins at 4°C, the pellet was resuspended in cell lysis buffer as per reported conditions, supplementing the cell lysis buffer with cytochalasin B (3 µg/ml) and rotating for 10 min at 4°C. Nuclei were pelleted at 300*g* for 10 mins at 4°C and subsequently processed following the reported protocol with the adjustment of adding cytochalasin B (3 µg/ml) into all solutions for chromatin preparation and sonication, antibody incubation, and wash steps. Chromatin was then sonicated for 15 cycles (30 s, high powder, 30-s pause, and 500-µl volume) in a water bath sonicator set at 4°C (Bioruptor 300. Diagenode, Denville, NJ). After centrifuging at 10,000*g* for 10 mins at 4°C, sheared chromatin was checked on agarose gel for a shear band comprised between ~150 and ~600 bp. Two micrograms of chromatin were kept for pooled input controls, whereas ~50 µg of chromatin was used for each pull-down reaction in a final volume of 2 ml rotating at 4°C overnight. Primary antibodies were as follows: rabbit poly-clonal anti-GR (#A2164, ABclonal), rabbit polyclonal anti-RNApol-II (A11181), mouse monoclonal ANTI-FLAG M2 (#F1804, Sigma-Aldrich, St. Louis, MO). Chromatin complexes were precipitated with 100 µl of Dynabeads M-280 (Sheep anti-mouse, # 11202D; sheep anti-rabbit, #11204; Thermo Fisher Scientific, Waltham, MA). After washes and elution, samples were treated with proteinase K (Cat# 19131, QIAGEN, Hilden, Germany) at 55°C, and cross-linking was reversed through overnight incubation at 65°C. DNA was purified using a MinElute purification kit (Cat# 28004, QIAGEN, Hilden, Germany) and quantitated using Qubit reader and reagents. Library preparation and sequencing were conducted at the NU Genomics Core, using TruSeq ChIP-seq library prep (with size exclusion) on ~10 ng of chromatin per ChIP sample or pooled inputs and HiSeq 50-bp was conducted using HOMER software (v4.10) after aligning fastq files to the mm10 mouse genome using bowtie2. PCA was conducted using ClustVis. Heatmaps of peak density were imaged with TreeView3. Peak tracks were imaged through WashU epigenome browser. Gene ontology pathway enrichment was conducted using the gene ontology analysis tool.

2-DG-6-phosphatase assay

For measuring the uptake of 2-DG-6-phosphatase, Glucose uptake-Glo^{TM} assay (Cat# J1341, Promega) was utilized to inject 1mM 2DG into mice for 30 mins before euthanasia. After 30 mins, the whole heart tissues were harvested and stored at -80C until ready to use. Next, the reagents from the kit were combined for reaction mixtures according to manufacturer's instructions and incubated at room temperature for 1 hr. The frozen heart

tissues were crushed into a fine powder and 20 - 50 mg of tissue powder was used for the assay. After 1 hour incubation of reaction mixture, 25 µl of Neutralization buffer was added to reaction mixture. Next, 125 µl of reaction mixture and neutralization buffer was added to powdered heart tissue and incubated for 1 hr. After incubation, the samples were centrifuged for 5 mins at 10,000*g* and 125 µl of the supernatant was loaded onto a 96-well plate for luminescence readings.

Respiratory on cardiomyocytes and isolated mitochondria

For cardiomyocytes, respiratory was performed on freshly isolated cells. Cardiomyocytes are isolated adapting to previously reported conditions. In anesthetized mice, the descending aorta is cut, and the heart is immediately flushed by injecting 7ml pre-warmed EDTA buffer into the right ventricle. Immediately afterwards, the ascending aorta is clamped using Reynolds forceps, the heart is removed and kept in the 60 mm dish with pre-warmed EDTA buffer. The digestion process is proceeded by injecting 10 ml pre-warmed EDTA buffer to the apex of left ventricle. The heart is then transferred to the 60 mm dish with perfusion buffer and 3 ml perfusion buffer is injected to flush out the EDTA buffer. Then the heart is transferred to another 60 mm dish with pre-warmed 180U/ml Collagenase II buffer and 30-40 ml collagenase buffer is injected into the apex of LV. Then the heart is cut from the clamp, the ventricular myocardial tissue is pulled gently into small pieces using forceps and further dissociated by gentle pipetting. The cardiomyocyte suspension is passed through a 200 µm mesh, and the digestion is stopped by adding 5ml of stop buffer. Cardiomyocytes are then centrifuged at 100*g* for 3 mins, resuspended in the stop buffer with increasing concentration of calcium (100 µM, 400 µM, and 1000 µM), re-centrifuged and then plated in laminin-coated Seahorse plates in culture media. After 1 h incubation, the culture media is aspirated and Seahorse media is added for respirometry, which starts after an additional 1 h equilibrium in a CO_2-free incubator. Buffer compositions: EDTA buffer contains 130 mM NaCl, 5mM KCl, 0.5mM NaH_2PO_4, 10mM HEPES, 10mM glucose, 10mM BDM, 10mM Taurine, 5 mM EDTA, pH 7.8; Perfusion buffer contains 130 mM NaCl, 5 mM KCl, 0.5 mM NaH_2PO_4, 10 mM HEPES, 10 mM glucose, 10 mM BDM, 10 mM taurine, 1 mM $MgCl_2$, pH 7.8; Collagenase buffer contains 220U/ml Collagenase II; Stop buffer consists of Perfusion buffer supplemented with 5% sterile fetal bovine serum; Culture medium (250 mL) contains 2.45g Hanks' salt, 5 mL non-essential amino acids, 2.5 mL MEM Vitamin Solution, 0.0875g $NaHCO_3$, 2.5 mL PenStrep 10X, 1 mg/mL bovine serum albumin. Regular seahorse protocol is followed with basal reads and injection of oligomycin, FCCP, Rotenone/Antimycin following reported conditions. Basal OCR was calculated as baseline value (average of 3 consecutive reads) minus value after rotenone/antimycin addition (average of 3 consecutive reads). Basal OCR values were normalized to total protein content, assayed in each well after the Seahorse ran through homogenization and Bradford assay. Mitochondrial ATP production rate was calculated as $OCR_{ATP} * 2$ (mol O in mol O_2) $*$ 2.75 (Seahorse P/O), where OCR_{ATP} is the difference between baseline and oligomycin OCR. Nutrients: 10 mM glucose or 10 mM pyruvate; inhibitors: 0.5 µM rotenone + 0.5 µM antimycin A (Agilent).

Respiratory control ratio (RCR) values were obtained from isolated mitochondria from myocardial tissue. Tissues from the left ventricle are harvested from the mouse and cut up into very fine pieces. The minced

tissue is placed in a 15 mL conical tube (USA Scientific #188261) and 5 mL of MS-EGTA buffer with 1 mg Trypsin (Sigma #T1426-50 MG) is added to the tube. The tube is quickly vortexed, and the tissue is left submerged in the solution. After 2 min, 5 mL of MS-EGTA buffer with 0.2% BSA (Goldbio #A-421-250) is added to the tube to stop the trypsin reaction. MS-EGTA buffer: Mannitol (#M0214-45, ChemProducts), Sucrose (#100892, Millipore), HEPES (#15630–080, Gibco), EGTA (#E14100–50.0, RPI). The tube is inverted several times to mix then set to rest. Once the tissue has settled to the bottom of the tube, 3 mL of buffer is aspirated, and the remaining solution and tissue is transferred to a 10 mL glass tissue homogenizer (Avantor # 89,026–382). Once sufficiently homogenized the solution is transferred back into the 15 mL conical tube and spun in the centrifuge at 1,000g for 5 min at 4 °C. After spinning, the supernatant is transferred to a new 15 mL conical tube. The supernatant in the new tube is then centrifuged at 12,000g for 10 min at 4 °C to pellet the mitochondria. The supernatant is discarded from the pellet and the pellet is then resuspended in 7 mL of MS-EGTA buffer and centrifuged again at 12,000g for 10 min at 4 °C. After spinning, the supernatant is discarded, and the mitochondria are resuspended in 1 mL of Seahorse medium (Agilent #103335–100) with supplemented 10 mM glucose (Sigma #G8270) or 5 mM pyruvate (Sigma #P2256-100G). After protein quantitation using a Bradford assay (Bio-Rad #5000001), 2.5 µg mitochondria are dispensed per well in 180 µl total volumes and let to equilibrate for 1 h at 37 degrees C. 20 µl of 5 mM ADP (Sigma #01905), 50 µM Oligomycin (Milipore #495455-10 MG), 100 µM Carbonyl cyanide-p-trifluoromethoxyphenylhydrazone (TCI #C3463), and 5 µM Rotenone (Milipore #557368-1 GM)/Antimycin A (Sigma #A674-50 MG) are added to drug ports A, B, and C, respectively. At baseline and after each drug injection, samples are read three consecutive times. RCR was calculated as the ratio between state III (OCR after ADP addition) and uncoupled state IV (OCR after oligomycin addition). All Seahorse measurements were conducted blinded to treatment groups.

Western blotting

Protein analyses in liver were performed on ~ 50 ug total lysates from the whole heart. Cyro-pulverized liver tissue was incubated in RIPA buffer (Cat #89900, Thermo Fisher Scientific, Waltham, MA) supplemented with 1x protease/phosphatase inhibitor (Cat #78440, Thermo Fisher Scientific, Waltham, MA) for 30 mins and sonicated for 10 secs twice. The samples were then centrifuged at 10,000 rpm for 10 mins at 4°C. Supernatant containing the protein is transferred into a new tube and used as a total lysate. For total cell lysates from culture cells, cells were harvested and resuspended in RIPA buffer containing 1x protease and phosphatase inhibitors. Lysates were incubated for 30 mins and centrifuged at 10,000 rpm for 10 mins at 4°C. The supernatant was used as a total cell lysate. The protein concentrations of the supernatants were determined using the Pierce BCA Protein Assay kit (Cat #23227, Thermo Fisher Scientific, Waltham, MA). Equal amounts of protein were separated using SDS-PAGE and transferred to a PVDF membrane (Cat #1620174, BioRad, Hercules, CA). Membranes were blocked in 5% milk in TBST for 1 hour at room temperature and then incubated overnight at 4°C with primary antibodies: Rabbit *Klf15* polyclonal antibody (Cat# A7194, ABclonal), Rabbit *Gapdh* monoclonal antibody (Cat# A10868, ABclonal), followed by incubation with HRP-conjugated secondary antibodies: Peroxidase AffiniPure Goat Anti-Rabbit IgG (H+L) (Cat# 111-035-003, Jackson

ImmunoResearch Labs, West Grove, PA) for 1 hour at room temperature. Immunoreactive bands were visualized by chemiluminescence using Pierce Enhanced Chemiluminescent western blotting substrate (Cat #32106, Thermo Fisher Scientific, Waltham, MA).

Echocardiography

Mice were anesthetized with 1.5% isoflurane (1.5% oxygen) and imaged in the supine position using Vevo 3100 Imaging System with a 35-MHz linear probe (Visualsonics, Canada). The core temperature was maintained at 37°C. Heart rates were kept consistent between the groups (400 – 450 bpm) [28]. The heart was imaged in a 2D, short axis, and 4-chamber view by placing the pulsed wave Doppler at the septal corner of the mitral annulus. Mitral inflow velocity (E) and longitudinal tissue velocity of the mitral anterior annulus (e') were measured through Vevo2100 1.5.0 Image Software [29].

Statistics

Statistical analyses were performed using Prism software v8.4.1 (Graphpad, La Jolla, CA). The Pearson-D'Agostino normality test was used to assess data distribution normality. When comparing two groups, tow-tailed Student's t-test with Welch's correction (unequal variances) was used. When comparing three groups of data for one variable, one-way ANNOVA with Sidak multi-comparison was used. When comparing data for more than one related variable, two-way ANOVA was used. For ANOVA and t-test analyses, a P value less than 0.05 was considered significant. When the number of data points was less than 10, data were presented as single values (dot plots, histograms). Tukey distribution bars were used to emphasize data range distribution in analyses pooling larger data points sets per group (typically >10 points). Analyses pooling data points over time were presented as line plots connecting medians of box plots showing distribution of all data per time point.

RESULTS

Comparing ZT0 vs ZT12 circadian times of intake, only ZT0 prednisone upregulates glucose-fueled cardiomyocyte respiration and pyruvate-fueled mitochondrial RCR

The glucocorticoid receptor is a major metabolic regulator, and pharmacological target. In the liver specifically, GR, controls both triglyceride and glucose metabolisms [30]. Furthermore, glucocorticoids are secreted with a predominant daily rhythm in humans, and in the early night in rodents [31]. To investigate the specific role of GR in the myocardium, considering its circadian oscillation, wild-type (WT) (C57BL/6J background) mice were treated with the glucocorticoid prednisone at ZT0 and harvested 24h post-injection for expression analysis. RNA-sequencing (RNAseq) data showed enrichment of pyruvate transport and glucose import (Figure 1A, left panel). Indeed, the light-phase glucocorticoid stimulation improves glucose uptake and oxidation in the heart. Enrichment analysis for Gene Ontology (GO) terms related to glucose and pyruvate revealed that intermittent prednisone administration at ZT0 increased the expression of key genes, including *Klf15*, *Adipor1*, *Mpc1*, and *Mpc2* in WT hearts treated with prednisone versus vehicle (Figure 1A, right panel). Notably, these expression trends were specific to ZT0 drug stimulation, apart from *Klf15,* as evidenced by their blunting with ZT12 intake (Figure 1B). In line with *Adipor1* upregulation, ZT0 prednisone treatment led to decreased myocardial ceramide

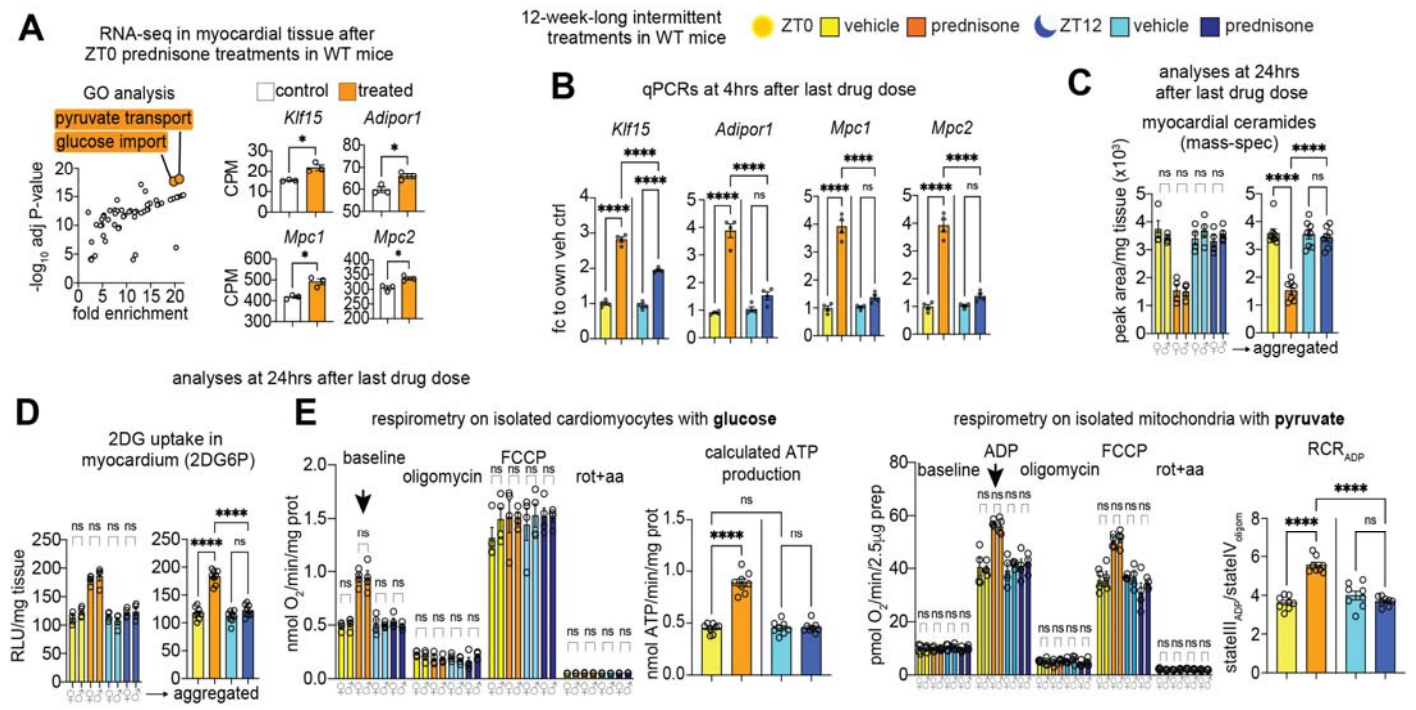

Figure 1. Light-phase glucocorticoid stimulation improves glucose uptake and oxidation in heart. (A) *Enrichment for GO terms related to glucose and pyruvate unveiled that ZT0 intermittent prednisone increased expression of Klf15, Adipor1, Mpc1 and Mpc2 in the WT heart.* ***(B)*** *These expression trends were specific to ZT0 drug stimulation, as they were blunted by ZT12 intake.* ***(C-D)*** *Consistent with Adipor1 upregulation, ZT0 prednisone treatment decreased myocardial ceramide abundance and increased insulin-dependent 2DG uptake in heart, independent from sex.* ***(E)*** *After ZT0 treatment, cardiomyocytes increased glucose-fueled respiration ex vivo (arrow), producing more ATP than control or ZT12 treatment. Consistent with Mpc1/2 upregulation ZT0 treatment increased ADP-stimulated respiration (arrow) and respiratory control ratio with pyruvate. These effects were sex independent. A: Welch's t-test; B-E: 2w ANOVA + Sidak; *, P<0.05; **, P<0.01; ***, P<0.001; ****, P<0.0001.*

abundance measured by mass spectrophotometry and increased insulin-dependent 2-deoxyglucose (2DG) uptake in the heart. This trends, were sex independent (Figure 1C-D). Moreover, ZT0 treatment induced a significant increase in glucose-fueled respiration *ex vivo* or at the cellular level (indicated by arrow), resulting in higher ATP production compared to control or ZT12 treatment. This trend was not observed with ZT12. Consistent with the upregulation of Mpc1/2, ZT0 treatment elevated ADP-stimulated respiration (arrow) and the respiratory control ratio with pyruvate. These effects were observed independent of sex (Figure 1E).

Light-phase prednisone increases similar recruitment of GR and Klf15 on the promoters (or genome wide) in heart

Given the critical role of KLF15 in cardiovascular metabolism, we selected it as a central point for our research to unravel its specific involvement to further understand the mechanistic interlink between glucocorticoid signaling and this transcription factor. The circadian rhythm-driven secretion of glucocorticoids, coupled with the metabolic regulatory functions of KLF15, prompted us to investigate the potential synergies or epigenetic interactions between these two components. By utilizing a heart specific tamoxifen inducible KLF15 ablation model, we intended to define the functional consequences of KLF15 loss in the heart and discern its impact on glucocorticoid-mediated gene programs at ZT0. This approach allowed us to gain insights into the specific roles of KLF15 and glucocorticoid receptor (GR) in shaping the cardiac metabolic landscape during the light phase. KLF15 is a GR target and co-factor [32]. Cardiomyocyte-specific KLF15 determines circadian transcriptomes and metabolic programs in heart [25] but the specific mechanisms for this role remain largely undetermined. To gain insight in this open question, we profiled GR and KLF15 epigenomic occupancy through ChIP-seq in myocardial tissue at 4-hours after a single pulse of light-phase prednisone, adapting the method we previously reported for muscle [33]. For KLF15, because no ChIP-seq-grade commercial antibodies are available, we used the KLF15-3xFLAG knock-in mice that Dr. Haldar (Amgen & UCSF) recently generated and reported [27], per-forming KLF15 immunoprecipitation through the FLAG tag.

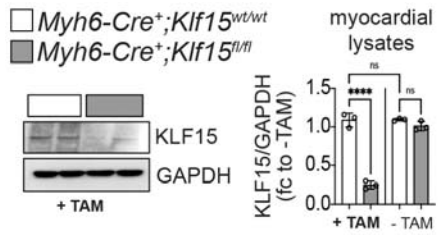

Figure 2. Validation of inducible KLF15 ablation in heart. *Compared to Cre^{+};Klf15$^{wt/wt}$ and non-tamoxifen controls, KLF15 was ~85% ablated by tamoxifen in Cre^{+}/Klf15$^{fl/fl}$ hearts. 2w ANOVA + Sidak; *, P<0.05; **, P<0.01; ***, P<0.001; ****, P<0.0001.*

Validating the functional consequences of inducible KLF15 ablation in the heart (Figure 2), we found that tamoxifen-induced ablation of KLF15 in Cre^{+}/Klf15$^{fl/fl}$ hearts was approximately 85% effective. Unbiased motif analysis (Figure 3A) validates the ChIP-seq datasets, illustrating the specificity of glucocorticoid receptor (GR) and Krüppel-like factor 15 (KLF15) binding to their

respective target genomic regions. Prednisone treatment induces a significant increase in the number of peaks and canonical epigenomic peak signals for both GR and KLF15 (Figure 3B). Notably, this effect occurs without altering their relative enrichment in genomic localization, with prevalent binding observed in promoter and 5'UTR regions for both factors. Principal Component Analysis (PCA) (Figure 3C) highlights distinct sample clustering patterns according to drug and genotype variables.

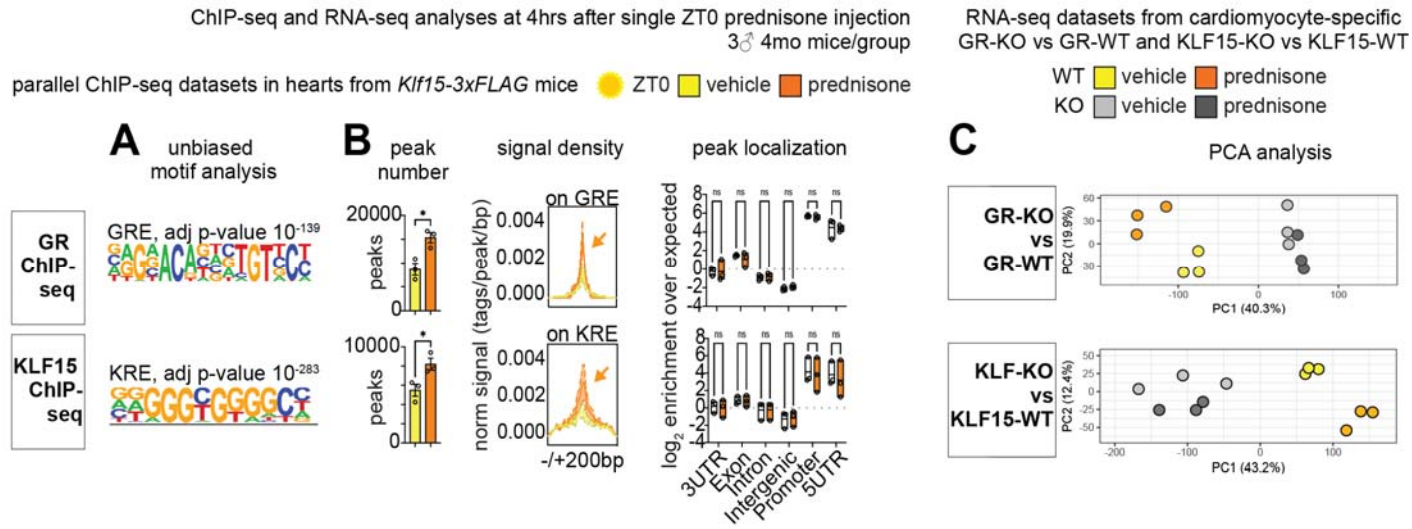

Figure 3. ChIP-seq and RNA-seq datasets reveal non-redundant mediator effect of both cardiomyocyte-specific GR and KLF15 on ZT0 glucocorticoid gene programs in heart. (A) *Validation of ChIP-seq datasets through unbiased motif analysis.* ***(B)*** *Prednisone increased peak numbers and canonical epigenomic peak signal (arrows) for both GR and KLF15 without changes in relative enrichment in genomic localization, which was prevalent in promoter and 5'UTRs for both factors.* ***(C)*** *PCA analyses show sample clustering according to drug and genotype variables. B: peak number, Welch's t-test; peak localization, 2w ANOVA + Sidak; *, P<0.05; **, P<0.01; ***, P<0.001; ****, P<0.0001.*

This underscores the non-redundant roles of both GR and KLF15 in orchestrating ZT0 glucocorticoid gene programs in the heart.

Cardiomyocyte GR and KLF15 regulate Adipor1 transactivation, ceramide reduction and insulin sensitization in heart during in the presence of glucocorticoids in ZT0

In order to gain insight into additional mechanisms enabled by cardiomyocyte-specific GR and KLF15 that could counteract the metabolic insults of diabetic cardiomyopathy, analogously to our reported cardiomyocyte-specific inducible *GR-KO* mice [14], for the *KLF15-KO* mice we crossed the *Myh6-MerCreMer* allele [34] with the floxed *Klf15* allele [25]. Our investigation into the roles of cardiomyocyte-specific glucocorticoid receptor (GR) and Krüppel-like factor 15 (KLF15) prednisone effects revealed their indispensable contributions to key metabolic processes in the heart in ZT0.

ChIP-seq analysis revealed steroid-sensitive peaks on the *Adipor1* transcription start site (TSS) for both for both GR and KLF15, emphasizing their involvement in the transactivation of *Adipor1* in response to prednisone treatment. Notably, the inducible cardiomyocyte-specific ablation of either *GR* or *KLF15* blunted the drug-induced upregulation of *Adipor1*, highlighting the non-redundant requirement of both transcription factors for ZT0 prednisone transactivation effects in the heart (Figure 4A).

Besides, our findings demonstrate that both GR and KLF15 are essential for the prednisone treatment effects on myocardial ceramide content reduction and insulin-stimulated glucose uptake in wild-type hearts (Figure 4B). The consistent trends observed in *Adipor1* expression are mirrored in the regulation of ceramide levels and glucose uptake, underscoring the interdependence of these

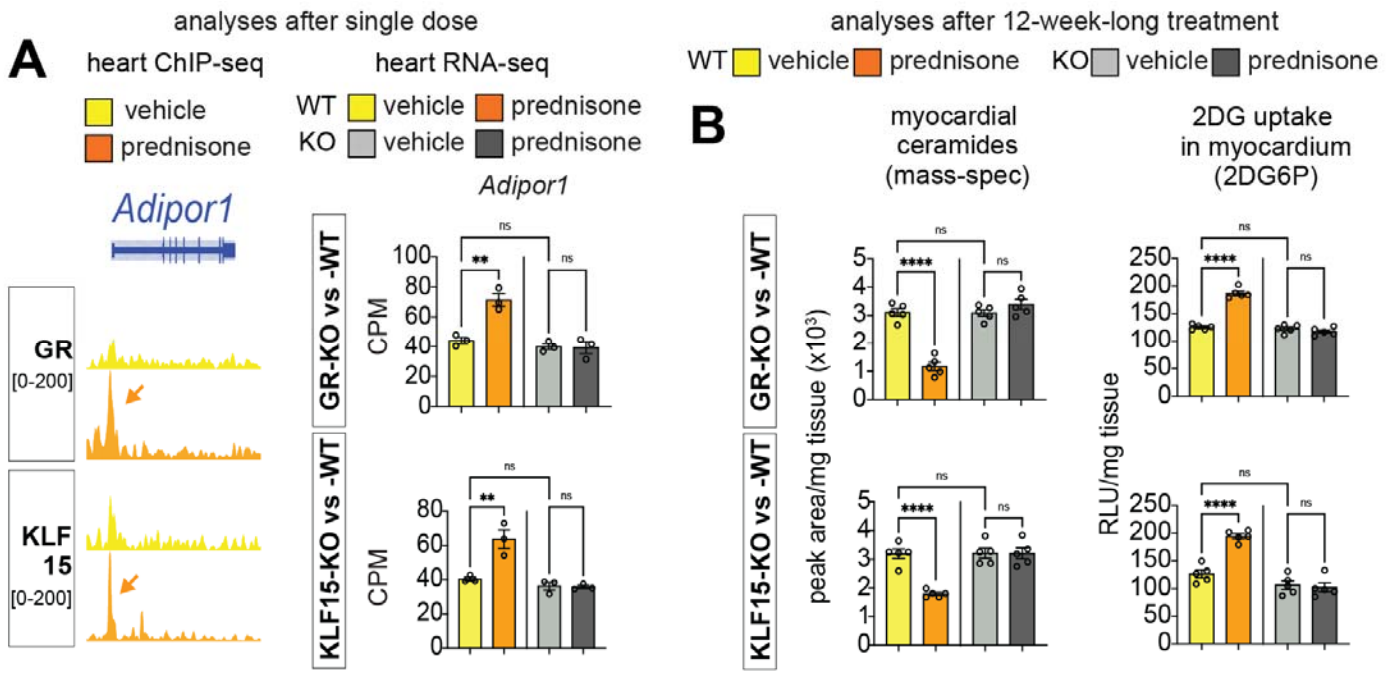

Figure 4. Cardiomyocyte GR and KLF15 are required for the ZT0 prednisone effects on Adipor1 transactivation, ceramide reduction and insulin sensitization in heart. (A) *GR and KLF15 showed steroid-sensitive peaks on Adipor1 TSS (arrows). Drug-induced upregulation was blunted by inducible cardiomyocyte-specific ablation of either GR or KLF15, demonstrating their non-redundant requirement for the ZT0 prednisone transactivation effect in heart.* ***(B)*** *Consistent with Adipor1 expression trends, GR and KLF15 were both required for the prednisone treatment effects on myocardial ceramide content reduction and insulin-stimulated glucose uptake increment in heart. 2w ANOVA + Sidak; *, P<0.05; **, P<0.01; ***, P<0.001; ****, P<0.0001.*

factors in mediating the metabolic response to ZT0 prednisone.

Cardiomyocyte GR and KLF15 are required Mpc1/2 transactivation and pyruvate oxidation in heart post prednisone treatment at ZT0

MPC expression is downregulated in failing human hearts [35] and transcriptional MPC abundance directly promotes cardioprotective oxidation of pyruvate and its precursor glucose in the myocardium [35-37]. We found that light-phase single prednisone shot in ZT0 activates GR and KLF15 epigenomic activity in heart (Figure 3), increasing its occupancy on the promoters of *Mpc1* and *Mpc2* (Figure 5A), encoding the two subunits of the mitochondrial pyruvate carrier (MPC). *Mpc1* and *Mpc2* upregulation by light-phase prednisone was not induced upon the ablation of GR or KLF15 in adult cardiomyocytes (Figure 5A). Since Mpc1/2 are required for pyruvate fueled mitochondrial respiration, mitochondria were isolated from WT vehicle *vs.* WT treated with prednisone, and of GR and KLF15 KO vehicle *vs.* KO prednisone and subjected to seahorse. we measured mitochondrial respiratory function through Seahorse-based respirometry in isolated mitochondria [38], quantitating respiratory control ratio (RCR) in isolated mitochondria. The RCR estimates the capacity of

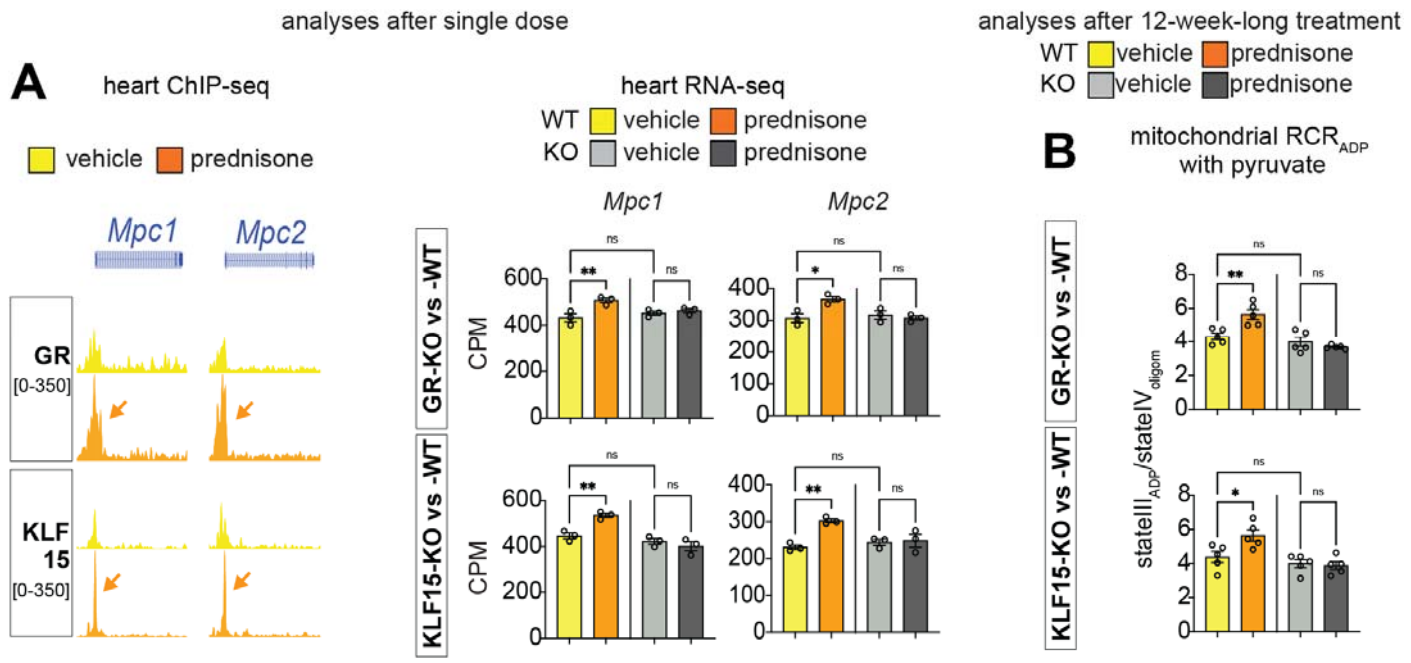

Figure 5. Cardiomyocyte GR and KLF15 are required for the ZT0 prednisone effects on Mpc1/2 transactivation and pyruvate oxidation in heart. (A) *GR and KLF15 showed steroid-sensitive peaks on both Mpc1 and Mpc2 TSS (arrows). Steroid-induced transactivation was blocked by inducible cardiomyocyte-specific ablation of either GR or KLF15.* ***(B)*** *Consistent with Mpc1/2 expression trends, GR and KLF15 were both required for the prednisone treatment effects on pyruvate oxidation increment in heart-derived isolated mitochondria. 2w ANOVA + Sidak; *, P<0.05; **, P<0.01; ***, P<0.001; ****, P<0.0001.*

isolated mitochondria to oxidize substrate to phosphorylate ADP and is indeed calculated as the ratio between state III (ADP) and state IV_o (oligomycin) OCR values [39]. Light-phase treatment increased mitochondrial RCR levels with pyruvate (Figure 5B) In concordance from our previous data. Pyruvate-fueled mitochondrial respiration was blocked by inducing GR or KLF15 ablation in adult mitochondria (Figure 5B).

ZT0 Intermittent glucocorticoid treatment rescues glucose oxidation and diastolic function in db/db mice

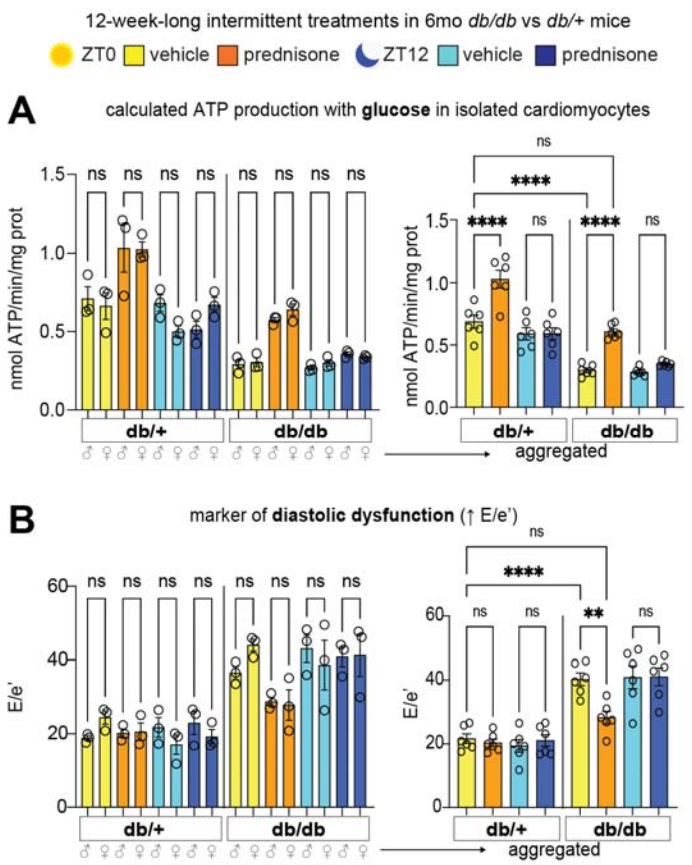

Figure 6. ZT0 glucocorticoid treatment rescues glucose oxidation and diastolic function in db/db mice. (A) *Treatment increased glucose-fueled ATP production calculated from Seahorse curves in isolated cardiomyocytes in both db/+ and db/db mice according to time of intake (ZT0), increasing db/db values to control-like levels.* ***(B)*** *Although no treatment effects were quantitated on E/e' values in db/+ controls, ZT0 prednisone decreased diastolic dysfunction to control-like levels, while the ZT12 treatment did not induce significant shifts. 3w ANOVA + Sidak; *, P<0.05; **, P<0.01; ***, P<0.001; ****, P<0.0001.*

To gather initial evidence of the functional relevance of light-phase-specific prednisone intermittence for the diabetic heart, we treated db/db mice (obese diabetic) at ~6 months of age for 12 weeks, using db/+ littermates as lean control. Db/db mice are a mutant model of severe type-2 diabetes [40] and related cardiomyopathy [41]. Compared to vehicle, treatment increased glucose-fueled basal respiration and ATP production calculated from the Seahorse curves in isolated cardiomyocytes, rescuing db/db levels to control-like. Similarly, to our previous data, these results were sex independent (Figure 6A). In live mice, treatment rescued diastolic dysfunction in db/db hearts to control-like levels, measured as E/A ratio through Doppler echocardiography [42] (Figure 5B). Despite these encouraging results, we still need to ascertain the extent to which the GR-KLF15 axis activation mediates the functional rescue we observed in diabetic hearts.

DISCUSSION

Glucocorticoids, as pharmacological agents are widely prescribed and used to treat cardiovascular pathologies, which vary from infectious disease such as myocarditis to structural and conduction cardiovascular disease such as vascular conditions, cardiomyopathy, or myocardial infarction [43]. Despite their wide use, the mechanism of action of GCs remains largely elusive, and long-term exposure to GCs has negative consequences [15, 44]. Thus, improving our knowledge on this topic will improve our drug development processes, enabling pathology modulation through different molecular effectors downstream GR.

While GR cardiomyocyte biology is still not fully understood, it has been reported that in premature cardiomyocytes, *in vitro*, GR is involved in cardiomyocyte maturation by promoting z-disc assembly and improve mitochondrial activity by regulating similar genes induced by Pgc1α *in vivo* [45]. Systemically, ZT0 prednisone improved mitochondrial metabolism rely significantly on GR and BMAL1 expression [14], whether GCs have a positive impact in murine disease models such as diabetic cardiomyopathy remains to be explored.

Firstly, we validated the time specific effects of GC treatment on the myocardium, particularly prednisone, revealing as we have shown previously [14], dependance on circadian timing. Indeed, our results show a significant difference between ZT0 and ZT12 prednisone treatment. This temporal specificity aligns with the endogenous secretion of glucocorticoids in physiological conditions. Notably, GR emerges once more as a key metabolism mediator in the heart, drawing parallels with its established role in the liver [46]. Whereas ZT0 prednisone single treatment upregulates glucose-fueled cardiomyocyte respiration, and pyruvate fueled mitochondrial respiratory control ratio (RCR), ZT12 single GCs injection had no significant effect. Previous studies in *epithelial-like* cells have already reported that GCs stimulate the expression of pyruvate dehydrogenase kinase 4 (PDK4), permitting the shift between glucose and fatty acid oxidation [47].

To gain insights on the molecular pathways that trigger metabolic changes through the administration of glucocorticoids, we performed epigenomic analysis. ChIP-seq experiments revealed coordinated actions of GR and KLF15 on promoters related to glucose and pyruvate metabolism. We found preliminary evidence for the adiponectin-sensitive ceramidase AdipoR1 and the mitochondrial carriers Mpc1/Mpc2 as novel cardiomyocyte GR and KLF15 targets. We then hypothesized that the cardiomyocyte GR-KLF15 axis rescues metabolic flexibility in the diabetic heart through a concerted program of ceramide reduction and pyruvate oxidation, dependent on timing-specific GC exposures.

In disease models, the study extends its findings to db/db mice, a model of severe type-2 diabetes [48]. ZT0 prednisone treatment rescues glucose-fueled basal respiration and diastolic function, providing initial evidence of potential therapeutic benefits for diabetic cardiomyopathy. Importantly, these effects are sex-independent, enhancing the generalizability of the results.

In summary, in this manuscript, we leveraged new circadian and metabolic mechanisms of GC biology to treat diabetic cardiomyopathy. Furthermore, we identified the zeitberg (ZT or timekeeper) through which GR treatment is effective. Finally, in contrast to the conventional of chronic GC triggering metabolic stress, we determined that GCs promote glucose and pyruvate metabolism by regulating Adipor1 and Mpc1/2 through GR and KLF15.

Acknowledgements - Mass-spec analyses were performed thanks to the Mass-Spec Metabolomics Core Facility at Robert H. Lurie Comprehensive Cancer Center of Northwestern University, with critical assistance by Dr. Gao. Next-gen sequencing was performed thanks to the Cincinnati Children's DNA Sequencing and Genotyping Facility (RRID: SCR_022630), with critical assistance by David Fletcher, Keely Icardi, Julia Flynn, and Taliesin Lenhart.

Grant support – This work was supported by R56HL158531-01, R01HL166356-01, R03DK130908-01A1, R01AG078174-01 (NIH) and RIP, CCRF Endowed Scholarship, HI Translational Funds (CCHMC) grants to MQ.

REFERENCES

[1] K.A. De Jong, G.D. Lopaschuk, Complex Energy Metabolic Changes in Heart Failure With Preserved Ejection Fraction and Heart Failure With Reduced Ejection Fraction, Can J Cardiol 33(7) (2017) 860-871.
[2] Q.G. Karwi, Q. Sun, G.D. Lopaschuk, The Contribution of Cardiac Fatty Acid Oxidation to Diabetic Cardiomyopathy Severity, Cells 10(11) (2021).
[3] D. Feuvray, J.A. Idell-Wenger, J.R. Neely, Effects of ischemia on rat myocardial function and metabolism in diabetes, Circ Res 44(3) (1979) 322-9.
[4] G.S. Gulsin, L. Athithan, G.P. McCann, Diabetic cardiomyopathy: prevalence, determinants and potential treatments, Ther Adv Endocrinol Metab 10 (2019) 2042018819834869.
[5] L. Athithan, G.S. Gulsin, G.P. McCann, E. Levelt, Diabetic cardiomyopathy: Pathophysiology, theories and evidence to date, World J Diabetes 10(10) (2019) 490-510.
[6] T.R. Einarson, A. Acs, C. Ludwig, U.H. Panton, Prevalence of cardiovascular disease in type 2 diabetes: a systematic literature review of scientific evidence from across the world in 2007-2017, Cardiovasc Diabetol 17(1) (2018) 83.
[7] N.J. Morrish, S.L. Wang, L.K. Stevens, J.H. Fuller, H. Keen, Mortality and causes of death in the WHO Multinational Study of Vascular Disease in Diabetes, Diabetologia 44 Suppl 2 (2001) S14-21.
[8] J.M. Berthiaume, J.G. Kurdys, D.M. Muntean, M.G. Rosca, Mitochondrial NAD(+)/NADH Redox State and Diabetic Cardiomyopathy, Antioxid Redox Signal 30(3) (2019) 375-398.
[9] Y.A. Chiao, A.D. Chakraborty, C.M. Light, R. Tian, J. Sadoshima, X. Shi, H. Gu, C.F. Lee, NAD(+) Redox Imbalance in the Heart Exacerbates Diabetic Cardiomyopathy, Circ Heart Fail 14(8) (2021) e008170.
[10] S.I. Oka, J. Byun, C.Y. Huang, N. Imai, G. Ralda, P. Zhai, X. Xu, S. Kashyap, J.S. Warren, J. Alan Maschek, T.S. Tippetts, M. Tong, S. Venkatesh, Y. Ikeda, W. Mizushima, T. Kashihara, J. Sadoshima, Nampt Potentiates Antioxidant Defense in Diabetic Cardiomyopathy, Circ Res 129(1) (2021) 114-130.
[11] R.H. Oakley, R. Ren, D. Cruz-Topete, G.S. Bird, P.H. Myers, M.C. Boyle, M.D. Schneider, M.S. Willis, J.A. Cidlowski, Essential role of stress hormone signaling in cardiomyocytes for the prevention of heart disease, Proc Natl Acad Sci U S A 110(42) (2013) 17035-40.
[12] R.H. Oakley, D. Cruz-Topete, B. He, J.F. Foley, P.H. Myers, X. Xu, C.E. Gomez-Sanchez, P. Chambon, M.S. Willis, J.A. Cidlowski, Cardiomyocyte glucocorticoid and mineralocorticoid receptors directly and antagonistically regulate heart disease in mice, Sci Signal 12(577) (2019).
[13] Y. Sainte-Marie, A. Nguyen Dinh Cat, R. Perrier, L. Mangin, C. Soukaseum, M. Peuchmaur, F. Tronche, N. Farman, B. Escoubet, J.P. Benitah, F. Jaisser, Conditional glucocorticoid receptor expression in the heart induces atrio-ventricular block, FASEB J 21(12) (2007) 3133-41.
[14] M. Wintzinger, M. Panta, K. Miz, A.D. Prabakaran, H.B. Durumutla, M. Sargent, C.B. Peek, J. Bass, J.D. Molkentin, M. Quattrocelli, Impact of circadian time of dosing on cardiomyocyte-autonomous effects of glucocorticoids, Mol Metab 62 (2022) 101528.
[15] M. Quattrocelli, A.S. Zelikovich, Z. Jiang, C.B. Peek, A.R. Demonbreun, N.L. Kuntz, G.D. Barish, S.M. Haldar, J. Bass, E.M. McNally, Pulsed glucocorticoids enhance dystrophic muscle performance through epigenetic-metabolic reprogramming, JCI Insight 4(24) (2019).
[16] A.S. Zelikovich, B.C. Joslin, P. Casey, E.M. McNally, S. Ajroud-Driss, An Open Label Exploratory Clinical Trial Evaluating Safety and Tolerability of Once-Weekly Prednisone in Becker and Limb-Girdle Muscular Dystrophy, J Neuromuscul Dis 9(2) (2022) 275-287.
[17] A.M. Curtis, Y. Cheng, S. Kapoor, D. Reilly, T.S. Price, G.A. Fitzgerald, Circadian variation of blood pressure and the vascular response to asynchronous stress, Proc Natl Acad Sci U S A 104(9) (2007) 3450-5.
[18] T. Seidel, D.J. Fiegle, T.J. Baur, A. Ritzer, S. Nay, C. Heim, M. Weyand, H. Milting, R.H. Oakley, J.A. Cidlowski, T. Volk, Glucocorticoids preserve the t-tubular system in ventricular cardiomyocytes by upregulation of autophagic flux, Basic Res Cardiol 114(6) (2019) 47.
[19] K.A. Lamia, S.J. Papp, R.T. Yu, G.D. Barish, N.H. Uhlenhaut, J.W. Jonker, M. Downes, R.M. Evans, Cryptochromes mediate rhythmic repression of the glucocorticoid receptor, Nature 480(7378) (2011) 552-6.
[20] H. Oster, S. Damerow, S. Kiessling, V. Jakubcakova, D. Abraham, J. Tian, M.W. Hoffmann, G. Eichele, The circadian rhythm of glucocorticoids is regulated by a gating mechanism residing in the adrenal cortical clock, Cell Metab 4(2) (2006) 163-73.
[21] C.B. Peek, A.H. Affinati, K.M. Ramsey, H.Y. Kuo, W. Yu, L.A. Sena, O. Ilkayeva, B. Marcheva, Y. Kobayashi, C. Omura, D.C. Levine, D.J. Bacsik, D. Gius, C.B. Newgard, E. Goetzman, N.S. Chandel, J.M.

Denu, M. Mrksich, J. Bass, Circadian clock NAD+ cycle drives mitochondrial oxidative metabolism in mice, Science 342(6158) (2013) 1243417.
[22] M.E. Young, R.A. Brewer, R.A. Peliciari-Garcia, H.E. Collins, L. He, T.L. Birky, B.W. Peden, E.G. Thompson, B.J. Ammons, M.S. Bray, J.C. Chatham, A.R. Wende, Q. Yang, C.W. Chow, T.A. Martino, K.L. Gamble, Cardiomyocyte-specific BMAL1 plays critical roles in metabolism, signaling, and maintenance of contractile function of the heart, J Biol Rhythms 29(4) (2014) 257-76.
[23] S. Gray, M.W. Feinberg, S. Hull, C.T. Kuo, M. Watanabe, S. Sen-Banerjee, A. DePina, R. Haspel, M.K. Jain, The Kruppel-like factor KLF15 regulates the insulin-sensitive glucose transporter GLUT4, J Biol Chem 277(37) (2002) 34322-8.
[24] L. Li, H. Li, C.L. Tien, M.K. Jain, L. Zhang, Kruppel-Like Factor 15 Regulates the Circadian Susceptibility to Ischemia Reperfusion Injury in the Heart, Circulation 141(17) (2020) 1427-1429.
[25] L. Zhang, D.A. Prosdocimo, X. Bai, C. Fu, R. Zhang, F. Campbell, X. Liao, J. Coller, M.K. Jain, KLF15 Establishes the Landscape of Diurnal Expression in the Heart, Cell Rep 13(11) (2015) 2368-2375.
[26] S.K. Sasse, C.M. Mailloux, A.J. Barczak, Q. Wang, M.O. Altonsy, M.K. Jain, S.M. Haldar, A.N. Gerber, The glucocorticoid receptor and KLF15 regulate gene expression dynamics and integrate signals through feed-forward circuitry, Mol Cell Biol 33(11) (2013) 2104-15.
[27] Z. Jiang, S.Z. Elsarrag, Q. Duan, E.L. LaGory, Z. Wang, M. Alexanian, S. McMahon, I.C. Rulifson, S. Winchester, Y. Wang, C. Vaisse, J.D. Brown, M. Quattrocelli, C.Y. Lin, S.M. Haldar, KLF15 cistromes reveal a hepatocyte pathway governing plasma corticosteroid transport and systemic inflammation, Sci Adv 8(10) (2022) eabj2917.
[28] M. Schnelle, N. Catibog, M. Zhang, A.A. Nabeebaccus, G. Anderson, D.A. Richards, G. Sawyer, X. Zhang, K. Toischer, G. Hasenfuss, M.J. Monaghan, A.M. Shah, Echocardiographic evaluation of diastolic function in mouse models of heart disease, J Mol Cell Cardiol 114 (2018) 20-28.
[29] E.M. Jeong, J. Chung, H. Liu, Y. Go, S. Gladstein, A. Farzaneh-Far, E.D. Lewandowski, S.C. Dudley, Jr., Role of Mitochondrial Oxidative Stress in Glucose Tolerance, Insulin Resistance, and Cardiac Diastolic Dysfunction, J Am Heart Assoc 5(5) (2016).
[30] F. Quagliarini, A.A. Mir, K. Balazs, M. Wierer, K.A. Dyar, C. Jouffe, K. Makris, J. Hawe, M. Heinig, F.V. Filipp, G.D. Barish, N.H. Uhlenhaut, Cistromic Reprogramming of the Diurnal Glucocorticoid Hormone Response by High-Fat Diet, Mol Cell 76(4) (2019) 531-545 e5.
[31] F. Spiga, J.J. Walker, J.R. Terry, S.L. Lightman, HPA axis-rhythms, Compr Physiol 4(3) (2014) 1273-98.
[32] S.K. Sasse, Z. Zuo, V. Kadiyala, L. Zhang, M.A. Pufall, M.K. Jain, T.L. Phang, G.D. Stormo, A.N. Gerber, Response Element Composition Governs Correlations between Binding Site Affinity and Transcription in Glucocorticoid Receptor Feed-forward Loops, J Biol Chem 290(32) (2015) 19756-69.
[33] M. Quattrocelli, M. Wintzinger, K. Miz, D.C. Levine, C.B. Peek, J. Bass, E.M. McNally, Muscle mitochondrial remodeling by intermittent glucocorticoid drugs requires an intact circadian clock and muscle PGC1alpha, Sci Adv 8(7) (2022) eabm1189.
[34] D.S. Sohal, M. Nghiem, M.A. Crackower, S.A. Witt, T.R. Kimball, K.M. Tymitz, J.M. Penninger, J.D. Molkentin, Temporally regulated and tissue-specific gene manipulations in the adult and embryonic heart using a tamoxifen-inducible Cre protein, Circ Res 89(1) (2001) 20-5.
[35] K.S. McCommis, A. Kovacs, C.J. Weinheimer, T.M. Shew, T.R. Koves, O.R. Ilkayeva, D.R. Kamm, K.D. Pyles, M.T. King, R.L. Veech, B.J. DeBosch, D.M. Muoio, R.W. Gross, B.N. Finck, Nutritional modulation of heart failure in mitochondrial pyruvate carrier-deficient mice, Nat Metab 2(11) (2020) 1232-1247.
[36] M. Fernandez-Caggiano, A. Kamynina, A.A. Francois, O. Prysyazhna, T.R. Eykyn, S. Krasemann, M.G. Crespo-Leiro, M.G. Vieites, K. Bianchi, V. Morales, N. Domenech, P. Eaton, Mitochondrial pyruvate carrier abundance mediates pathological cardiac hypertrophy, Nat Metab 2(11) (2020) 1223-1231.
[37] Y. Zhang, P.V. Taufalele, J.D. Cochran, I. Robillard-Frayne, J.M. Marx, J. Soto, A.J. Rauckhorst, F. Tayyari, A.D. Pewa, L.R. Gray, L.M. Teesch, P. Puchalska, T.R. Funari, R. McGlauflin, K. Zimmerman, W.J. Kutschke, T. Cassier, S. Hitchcock, K. Lin, K.M. Kato, J.L. Stueve, L. Haff, R.M. Weiss, J.E. Cox, J. Rutter, E.B. Taylor, P.A. Crawford, E.D. Lewandowski, C. Des Rosiers, E.D. Abel, Mitochondrial pyruvate carriers are required for myocardial stress adaptation, Nat Metab 2(11) (2020) 1248-1264.
[38] T.K. Sato, S. Panda, L.J. Miraglia, T.M. Reyes, R.D. Rudic, P. McNamara, K.A. Naik, G.A. FitzGerald, S.A. Kay, J.B. Hogenesch, A functional genomics strategy reveals Rora as a component of the mammalian circadian clock, Neuron 43(4) (2004) 527-37.
[39] S. Sakamuri, J.A. Sperling, V.N. Sure, M.H. Dholakia, N.R. Peterson, I. Rutkai, P.S. Mahalingam, R. Satou, P.V.G. Katakam, Measurement of respiratory function in isolated cardiac mitochondria using Seahorse XFe24 Analyzer: applications for aging research, Geroscience 40(3) (2018) 347-356.

[40] D.L. Coleman, Obese and diabetes: two mutant genes causing diabetes-obesity syndromes in mice, Diabetologia 14(3) (1978) 141-8.
[41] L. Alex, I. Russo, V. Holoborodko, N.G. Frangogiannis, Characterization of a mouse model of obesity-related fibrotic cardiomyopathy that recapitulates features of human heart failure with preserved ejection fraction, Am J Physiol Heart Circ Physiol 315(4) (2018) H934-H949.
[42] S.K. Saha, A. Kiotsekoglou, N.C. Nanda, Echocardiography 2020: Toward deciphering the "Rosetta stone" of left ventricular diastolic function, Echocardiography 37(11) (2020) 1886-1889.
[43] U. Nussinovitch, J.F. de Carvalho, R.M. Pereira, Y. Shoenfeld, Glucocorticoids and the cardiovascular system: state of the art, Curr Pharm Des 16(32) (2010) 3574-85.
[44] A.M. Connolly, J. Schierbecker, R. Renna, J. Florence, High dose weekly oral prednisone improves strength in boys with Duchenne muscular dystrophy, Neuromuscul Disord 12(10) (2002) 917-25.
[45] E.A. Rog-Zielinska, M.A. Craig, J.R. Manning, R.V. Richardson, G.J. Gowans, D.R. Dunbar, K. Gharbi, C.J. Kenyon, M.C. Holmes, D.G. Hardie, G.L. Smith, K.E. Chapman, Glucocorticoids promote structural and functional maturation of foetal cardiomyocytes: a role for PGC-1alpha, Cell Death Differ 22(7) (2015) 1106-16.
[46] S.M. Praestholm, C.M. Correia, L. Grontved, Multifaceted Control of GR Signaling and Its Impact on Hepatic Transcriptional Networks and Metabolism, Front Endocrinol (Lausanne) 11 (2020) 572981.
[47] S. Connaughton, F. Chowdhury, R.R. Attia, S. Song, Y. Zhang, M.B. Elam, G.A. Cook, E.A. Park, Regulation of pyruvate dehydrogenase kinase isoform 4 (PDK4) gene expression by glucocorticoids and insulin, Mol Cell Endocrinol 315(1-2) (2010) 159-67.
[48] P.C. Guest, H. Rahmoune, Characterization of the db/db Mouse Model of Type 2 Diabetes, Methods Mol Biol 1916 (2019) 195-201.